Optical Pumping of Rubidium Atoms to Explore Electronic Fine Structure and Transient Ringing Effects

Ian Brown and Yueze Liu

July 2022

1 Abstract

The hyperfine splitting of the ^{87}Rb and ^{85}Rb spectra is analyzed using an optical pumping setup that pumps electrons into the $^2S_{1/2}, F = 1, m_F = 2$ Zeeman state. Resonances between the optically pumped state and lower-m_F states allow the Rb fine structure (as a function of magnetic field) to be probed by a low-amplitude radio frequency (RF) magnetic field. The magnitude of the Zeeman splitting is observed to conform to the shape described by the Breit-Rabi equation [1], in both the linear and quadratic regimes. Lastly, a transient ringing effect that occurs as a response of the pumped state to the resonant RF magnetic field, modulated by a square waveform, is investigated.

2 Introduction

As electrons in an atom absorb photons, they undergo transitions to higher energy levels. Unless it is perturbed in some way, such an excited atom will tend towards an equilibrium state by reemitting photons. In this lab, we explore the properties of a non-equilibrium, metastable state, known as optical pumping. Optical pumping is a process that uses the properties of circularly polarized light along with fine structure splitting to concentrate electrons in an excited energy level.

2.1 How Optical Pumping Works

Circularly polarized light is known to have angular momentum. When circularly polarized photons are absorbed by electrons, the angular momentum of the system must be conserved, meaning that the angular momentum of the electrons must increase. However, the available electronic states are dictated by the structure of the atomic orbitals, meaning that there may not be any higher angular-momentum states for the electrons to transition into. When this is the case, the electrons in a sample that is irradiated with circularly polarized light will concentrate into a state that maximizes the angular momentum of the system. This phenomenon is known as optical pumping.

As can be seen in Figure 1, electrons are excited into the $^2P_{1/2}$ state by the circularly polarized pumping light. As these electrons relax back into the ground state, some will relax into the aforementioned $m_F = 2$ state. Electrons in this state cannot absorb the circularly polarized light, causing electrons to build up in this state. This buildup is further visualized in Figure 2: when the pumping light is on, electrons stochastically move between the states until they get "stuck" in the $m_F = 2$ state.

It should be noted that the electrons in the $m_F = 2$ state can emit low-energy, circularly polarized photons to relax into a lower-m_F state, however, once this occurs, the electrons in the lower-m_F states are pumped once again to the $m_F = 2$ state. This behavior can be modeled with a rate equation, as is described in Equation (1):

$$\frac{dp_k}{dt} = -\sum_{j=1,\ j\neq k}^{8}(b_{kj} + w_{kj})p_k + \sum_{i=1,\ i\neq k}^{8}(b_{ik} + w_{ik})p_i \tag{1}$$

where $k \in \{0, 1, 2, ..., 8\}$ is the number of the level, p_k is the occupation probability of the k-th level, b_{ij} is the probability per unit time that an electron has undergone a transition between the i-th and j-th states through the absorption and re-emmision of a photon, and w_{ij} is the probability per unit time of the electron relaxing into a lower-m_F state.

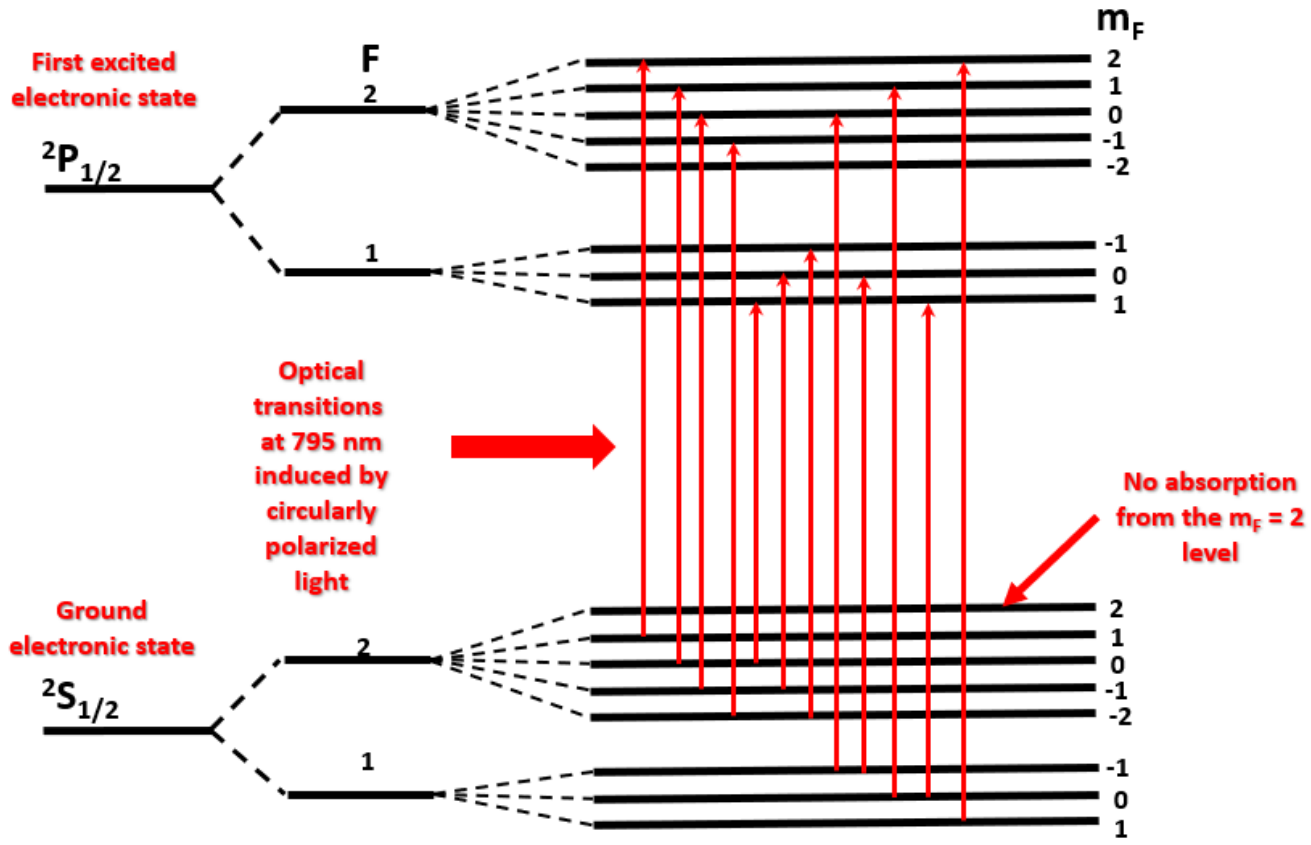

Figure 1: Optical pumping into the $^2S_{1/2}, F = 1, m_F = 2$ state

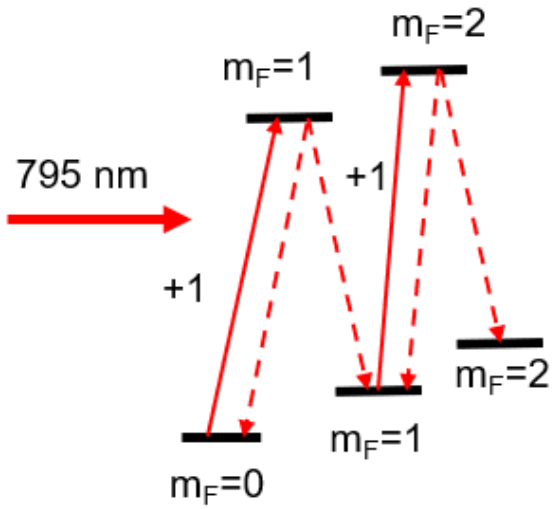

Figure 2: The pumping process stochastically concentrates electrons into the $m_F = 2$ state

2.2 Zero Field Transition

The m_F levels have different energies only when the atom is coupled to an external magnetic field. As the magnetic field approaches zero, the m_F levels become degenerate, causing optical pumping to break down, which in turn w_{kj} to increase. Thus, as the external magnetic field approaches zero, the sample can absorb more pumping light. In the presence of a magnetic field, the pumping light would have passed right through the sample due to there being no available states for the electrons in the $m_F = 2$ state to jump to. This effect, known as the zero-field transition, is used to calibrate the setup against the Earth's magnetic field (See Section 3.2.1).

2.3 Zeeman Effect

The Zeeman Effect describes how the spectrum of an element splits when the it is subjected to an external magnetic field. The splitting is due to the breaking of the degeneracy in the m_F sublevels. Since m_F describes the component of the atomic magnetic moment along the external B field, the energy of that sublevel will increase with B if m_F is positive, and vice versa. The magnitude of this splitting with respect to the magnitude of the external field is given by the Breit-Rabi equation:

$$W(F, M) = -\frac{\Delta W}{2(2I+1)} - \frac{\mu_I}{I} BM \pm \frac{\Delta W}{2}(1 + \frac{4M}{2I+1}x + x^2)^{1/2} \tag{2}$$

where $x = (g_J - g_I)\frac{\mu_0 B}{\Delta W}$ and

W = interaction energy between the atom and the field
F = total angular momentum quantum number
ΔW = hyperfine energy splitting
I = nuclear spin quantum number
μ_I = nuclear magneton
B = external magnetic field
M = component of atomic magnetic moment parallel to B (azimuthal quantum number)
μ_0 = magnetic susceptibility of free space
g_J = electronic g-factor (see Section 3.2.2)
$g_I = -\frac{\mu_I}{I\mu_0}$ = nuclear g-factor

Figure 3 shows a plot of Equation (2). There are three regimes of interest in this graph: a linear region corresponding to a small, perturbative magnetic field, a quadratic region where the electronic and nuclear magnetic moments become decoupled, and a third, linear region where the nuclear magnetic moment has been completely decoupled from the electronic magnetic moment. The first linear and quadratic regimes were investigated in this experiment.

2.4 Transients

Consider a case where optical pumping has brought the electrons into the metastable $m_F = 2$ state, and then RF field (whose frequency is equal to the Larmor frequency of the Rb atoms in the main field) is suddenly turned on. To analyze this problem, it is helpful to isolate the effect of the RF field on the atoms by considering it from a reference frame that follows the precession of the atomic angular momenta about the main field (see Figure 4). This precession is described by Equation (3):

$$\frac{d\mathbf{F}}{dt} = \gamma \mathbf{F} \times \mathbf{B} \tag{3}$$

where $\gamma\mathbf{F}$ is the atomic magnetic moment, $\mathbf{B}$ is the external magnetic field, and $\frac{d\mathbf{F}}{dt}$ is the torque exerted by the magnetic field on the atom. To consider the effect of the RF magnetic field, we change into a rotating reference frame:

$$\frac{d\mathbf{F}}{dt} = \frac{\partial \mathbf{F}}{\partial t} + \omega \times \mathbf{F} \tag{4}$$

where $\mathbf{F}$ represents the atomic angular momentum, and ω is the angular velocity of the frame. Combining equations 3 and 4, we derive the following:

$$\frac{\partial \mathbf{F}}{\partial t} = \gamma \mathbf{F} \times \mathbf{B}_{eff} \tag{5}$$

where $\mathbf{B}_{eff} = \mathbf{B} + \frac{\omega}{\gamma}$. As can be seen in Equation 5, the atomic angular momentum will precess around $\mathbf{B}_{eff}$ in the rotating frame. Taking $\mathbf{B} = \mathbf{B}_{main} + \mathbf{B}_{RF}$, we can calculate the magnitude of the effective magnetic field in the rotating frame:

$$||B_{eff}|| = (||B_{main} - \frac{\omega}{\gamma}||^2 + ||B_{RF}||^2)^{\frac{1}{2}} \tag{6}$$

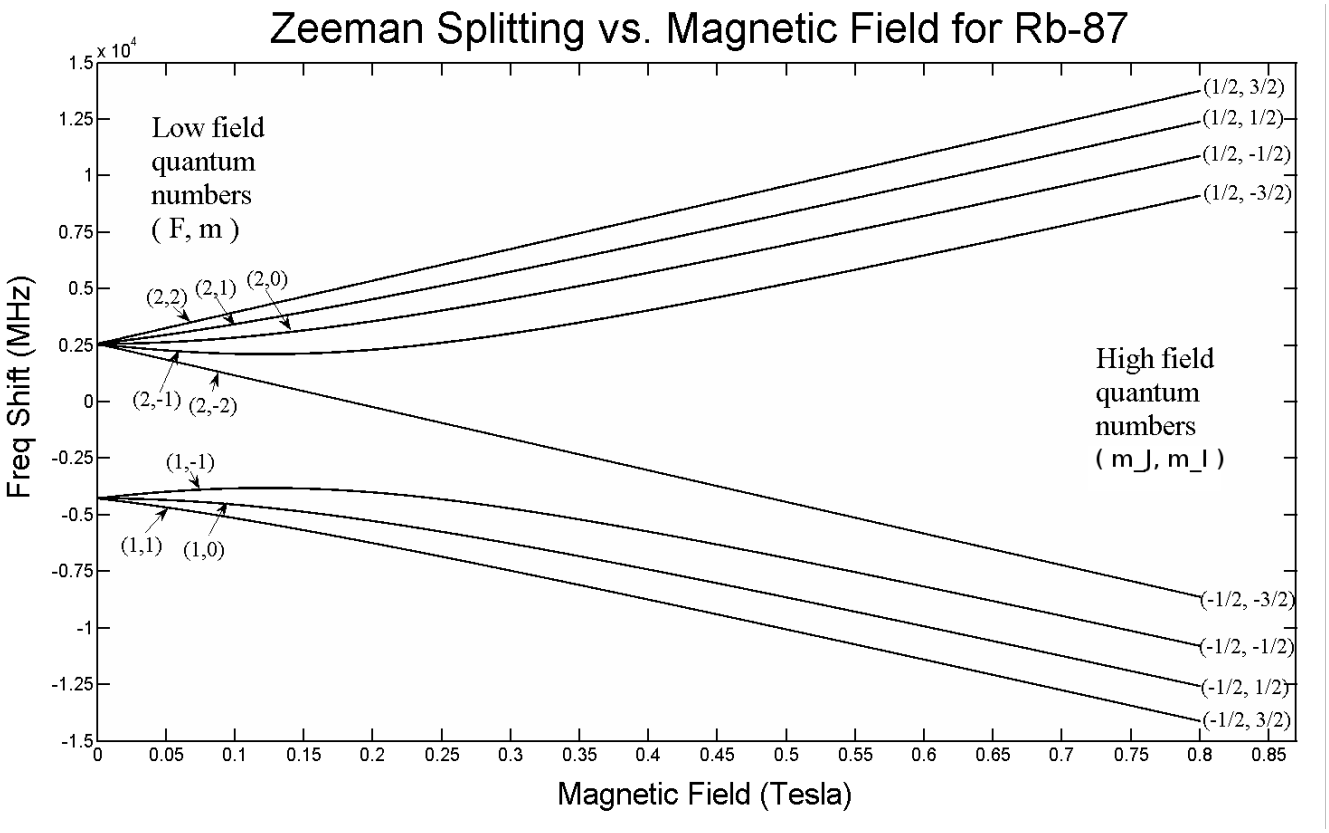

Figure 3: Breit-Rabi diagram showing the Zeeman splitting as a function of magnetic field

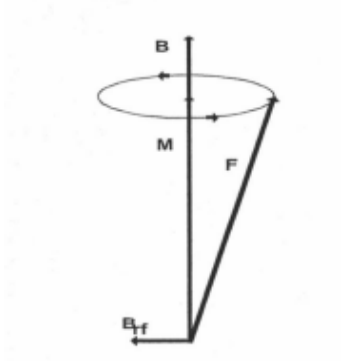

Figure 4: Precession of F, the atomic angular momentum, about the main field, B

Figure 5: As the RF field oscillates back and forth, the procession direction of F in the rotating frame changes

By taking ω to be equal to γB_{main}, the Larmor frequency of the oscillations about $\mathbf{B}_{main}$, $\mathbf{F}$ will precess around $\mathbf{B}_{RF}$ in the rotating frame with frequency $\nu = \gamma B_{RF}$. Since $\nu << \omega$, the period of $\mathbf{F}$'s precession around $\mathbf{B}_{RF}$ is much longer than the period of $\mathbf{B}_{RF}$ itself. This gives $\mathbf{F}$ a metronome-like motion in the rotating frame (see Figure 5). As $\mathbf{F}$ oscillates in this way, M, the azimuthal quantum number, which can be thought of as the projection of $\mathbf{F}$ onto $\mathbf{B}_{main}$, shifts between $M = 2$ and $M = 1$ with a frequency of 2ω. As $\mathbf{B}_{RF}$ moves the electrons into the $M = 1$ state, some are pumped back into the $M = 2$ state by the pumping light. Furthermore, when the electrons are in the $M = 2$ state, they can relax into the $M = 1$ state via nuclear relaxation processes. These processes, along with inhomogeneity in $\mathbf{B}_{RF}$ eventually distribute the electrons between the $M = 1$ and $M = 2$ states. The time constant of these processes is given in [2]:

$$\frac{1}{T_2^*} = \frac{1}{T_r} + \frac{1}{T_2} + \gamma \Delta B_{RF} \tag{7}$$

where T_2^* is the total time constant of the distribution, T_r is the time constant of the nuclear relaxation processes, T_2 is the time constant of the pumping, and ΔB_{RF} is the inhomogeneity of the RF field.

As soon as the B_{RF} is turned on, the distribution of electrons among the $M = 1$ and $M = 2$ states will combine with the effects of B_{RF} to create a damped ringing signal in the transmitted light intensity that is described by Equation (8):

$$I \propto \exp\left(-t/T_2^*\right) \cos(2\gamma B_{RF} t) \tag{8}$$

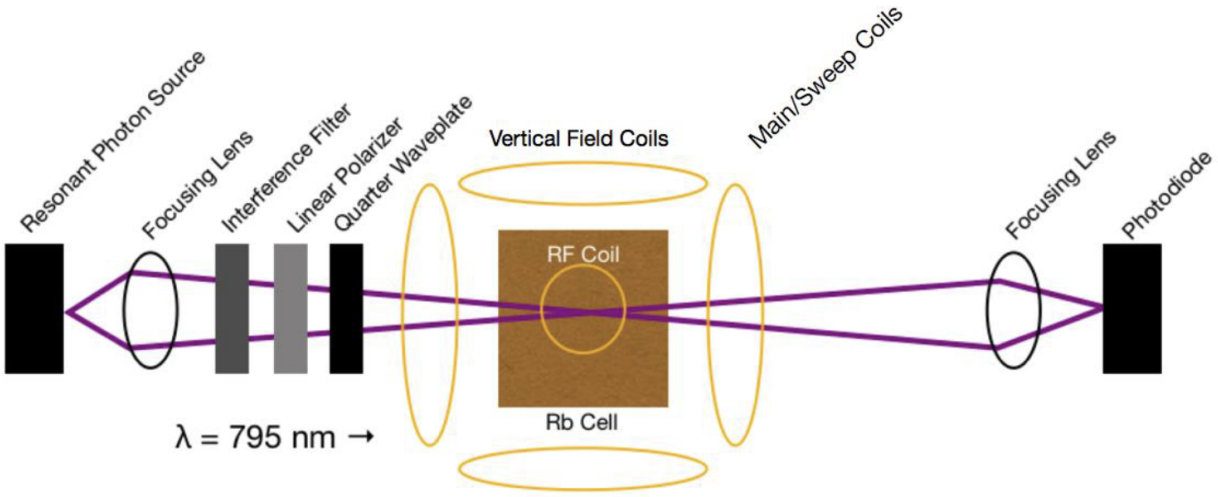

Figure 6: Visualization of the optical pumping experimental setup

3 Methodology

3.1 Equipment

The primary components of the experimental setup were a resonant photon source, polarizer, quarter-wave plate, Rb sample, photodiode, and a set of coils to control the magnetic field on the sample. A basic diagram of the setup can be seen in Figure 6.

The purpose of the resonant photon source was to emit photons of a frequency that would induce transitions between the ${}^2S_{1/2}$ and ${}^2P_{1/2}$ states. This light was then circularly polarized by the linear polarizer and quarter-wave plate, giving it a positive angular momentum. The light then passed through the sample, where it was then absorbed to the degree necessitated by the sample's state, as outlined in Section 2. This absorption (or the lack thereof) was then measured by the photodiode and sent to a computer for processing.

The setup was placed on a table that could be moved to align the apparatus with the Earth's magnetic field. Additional field calibration was done with the vertical and main field coils, effectively neutralizing the effect of Earth's magnetic field. The setup was covered with a shroud to prevent interference from photons coming from the ambient environment (see Figure 7).

3.2 Calibration

3.2.1 Aligning Against the Earth's Magnetic Field

The Earth's magnetic field can be thought to have two components: one parallel to the floor and one perpendicular. As seen in Figure 7, the entire setup was placed on a movable table to allow for alignment with the component parallel to the floor. A vertical coil was used to negate the effect of the vertical component of the Earth's magnetic field.

Horizontal Component To align the table with the horizontal component of the Earth's magnetic field, we observed the width of the zero-field transition over a sweep of main field values. We modified the direction of the table until the width of this transition was minimized.

Vertical Component The procedure to align the vertical component of the magnetic field is very similar to that of the horizontal field. Instead of turning the table, however, we increased the vertical field amperage until the width of the zero-field transition was minimized.

Figure 7: The setup was mounted on a movable table to allow for alignment with the Earth's magnetic field

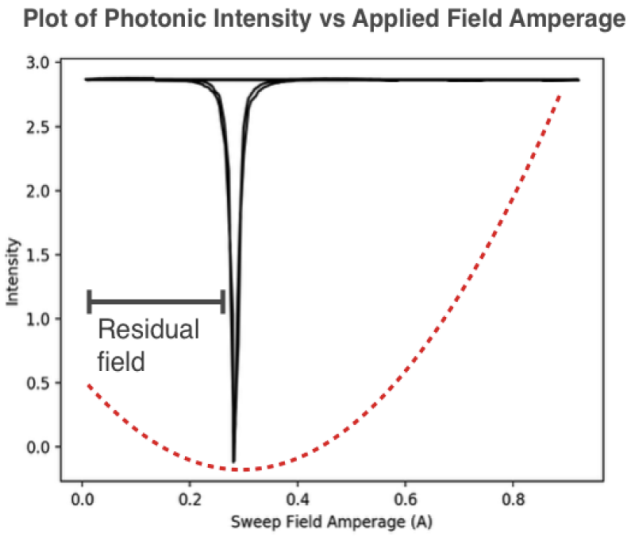

Figure 8: Minimal width of the zero-field transition corresponds to alignment with the earth's magnetic field

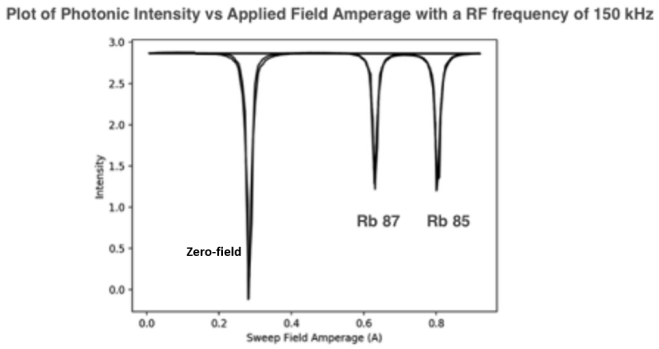

Figure 9: Linear Zeeman effect data points were collected by holding ν constant and sweeping the magnetic field

3.2.2 Calibrating Main Field and Sweep Field Coils

Measuring g_F for ^{87}Rb and ^{85}Rb It is known that the atomic g-factor, g_F is $\frac{1}{2}$ for ^{87}Rb and $\frac{1}{3}$ for ^{85}Rb. We will use this fact, along with the linear Zeeman effect, to calibrate the magnetic field in the sweep coil and main coil (see Figure 6). This calibration is equivalent to solving for the coefficient α in the equation $B = \alpha I$, where B is the magnetic field strength in the sample, and I is the current in the coil. The linear Zeeman effect is given by Equation (9):

$$\nu = g_F \mu_0 B(I)/h \tag{9}$$

where ν is the transition frequency between two Zeeman sublevels, $B(I)$ is the magnetic field strength (as a function of current), and h is Planck's constant. To measure g_F, we assume the $B(I)$ is given by the solenoid equation, $B(I) = 8.991 \times 10^{-3} IN/R$, where $N = 11$ is the number of turns per side, and $R = 0.1639$m is the mean radius. We extracted approximate values for g_F by plotting ν against this value for $B(I)$ (see Figure 10 and Table 1).

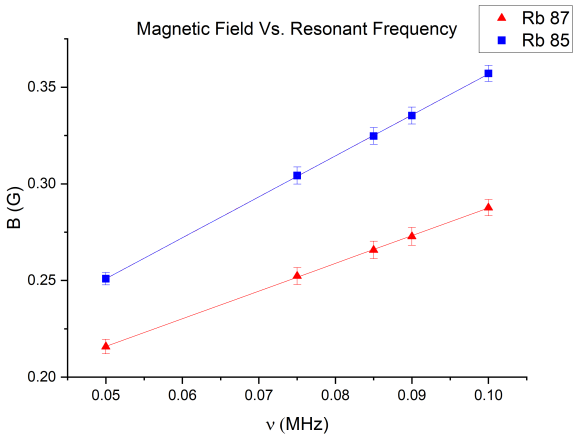

Figure 10: Linear Zeeman Relationship for ^{85}Rb and ^{87}Rb

Isotope	Linear Regression Equation	g_F (Calculated)
^{85}Rb	$B = 0.145 + 2.118\nu$	0.337
^{87}Rb	$B = 0.144 + 1.432\nu$	0.495

Table 1: Calculation of g_F based on estimated B field

Calibration of Sweep and Main Coils To calibrate the sweep and main coils, we took g_{F87} to be exactly $\frac{1}{2}$. We then rescaled B accordingly based on this assumption, giving us an exact calibration for B_{sweep} and B_{main} as a function of current.

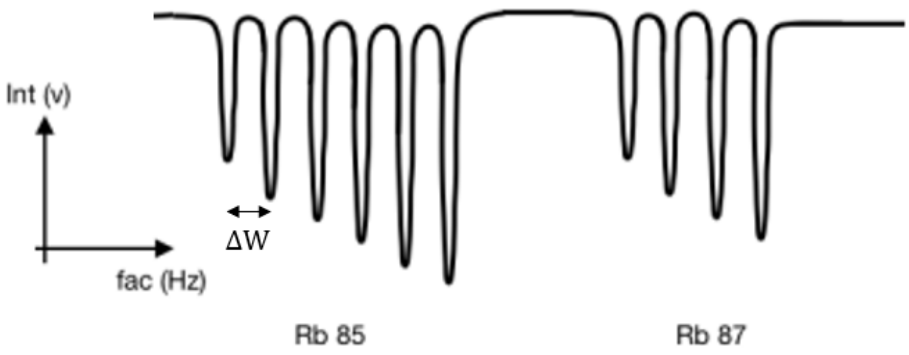

Figure 11: Sweeping the RF frequency allows for each m_F transition to be observed

3.3 Measuring Quadratic Zeeman Effect Using RF Spectroscopy

When measuring the linear Zeeman Effect, each data point was found by varying the magnitude of the sweep field while holding the RF frequency constant, then recording the fields at which absorption peaks were produced. To measure the quadratic Zeeman effect, the opposite approach was used: for each data point, the B field was held constant while the RF frequency was swept. This allows for the transitions between each m_F sublevel to be distinguished (see Figure 11). The resonant frequencies at which transitions occurred were recorded, then ΔW, the magnitude of the splitting, was calculated by averaging the distance between the peaks for the ^{85}Rb spectrum. This procedure was repeated for several different values of the main magnetic field.

3.4 Measuring Transients

To measure the transient effects, the RF field was modulated by a square wave which periodically turned the RF field on and off. The modulation was intended to occur on a timescale larger than that of the pumping and decay times, allowing the electrons to settle in both the pumped and thermodynamic equilibria, depending on the position in the cycle. The intensity of the transmitted light was observed with respect to time as this modulation was occurring. We then varied the intensity of the RF field to observe how it affected the period of the ringing. Assuming Equation (8) correctly describes the physics of the situation, then the period of the ringing will be inversely related to B_{RF}.

4 Results and Discussion

4.1 Quadratic Zeeman Effect

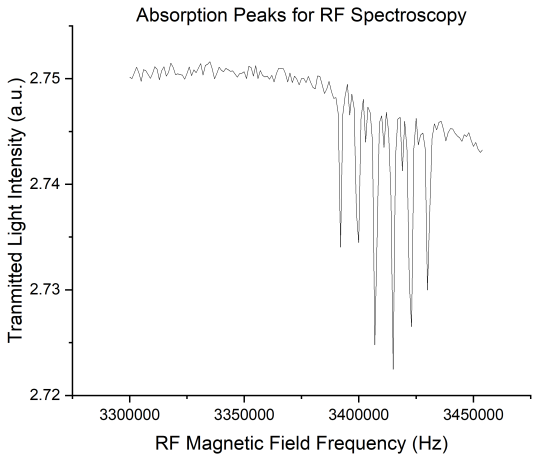

Figure 12: Absorption Peaks for $I_{main} = 0.85A$

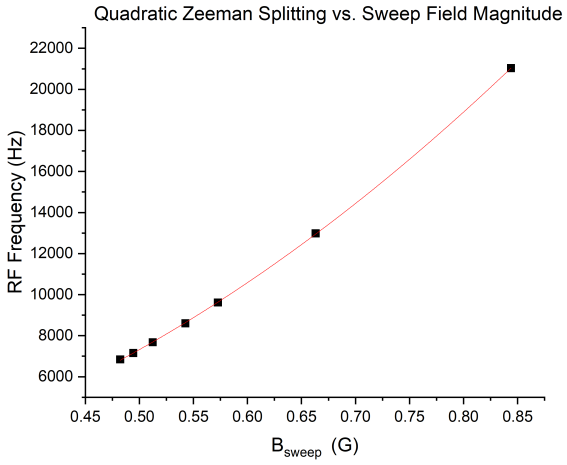

Figure 13: Magnitude of the Zeeman splitting with respect to B_{sweep}

Equation	$\nu = \alpha + \beta B_{sweep} + \gamma B_{sweep}^2$
α	-66 ± 442 Hz
β	-95 ± 1387 Hz/G
γ	29742 ± 1044 Hz/G^2

Table 2: Fit for Quadratic Zeeman Splitting

As can be seen in Figure 13, a quadratic relationship was found between the magnetic field, B_{sweep} and the distance between the Zeeman absorption frequencies. This verifies the prediction made by the Breit-Rabi formula (Equation (2)) that the splitting will be quadratic for sufficiently high B.

4.2 Transients

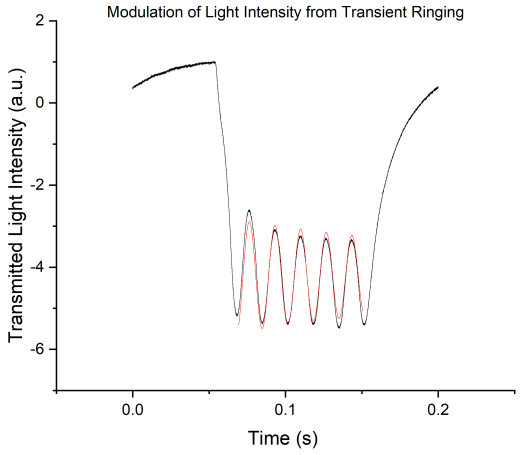

Figure 14: Transient ringing effect for $V_{RF} = 3.5$ V

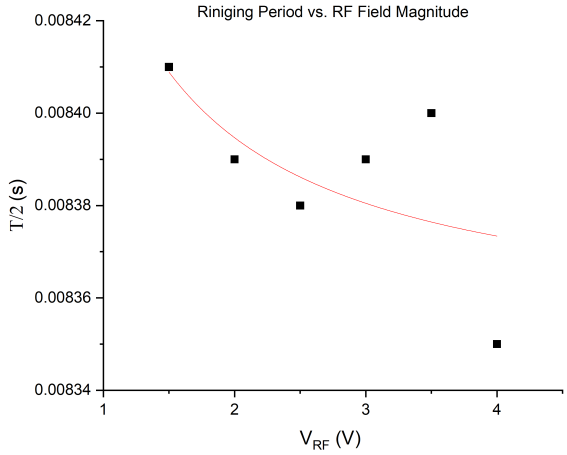

Figure 15: Ringing Period vs. RF Field Magnitude

Equation	$T/2 = \alpha + \beta/V_{RF}$
α	0.00835 ± 0.00002 s
β	0.0000853 ± 0.0000509 s $\cdot$ V

Table 3: Rational Fit for Transient Ringing Period

The data collection for the transient effects left much to be desired. As shown in Figure 14, the ringing did not die out before the RF was switched off. This begs the question whether other effects that sustained the ringing could have been involved. A primary candidate is poor calibration of the setup: it was essential to place the system at the bottom of one of the transition peaks, but if the auto-calibrator did not do this correctly, unforeseen coupling with the RF magnetic field could have affected the transmitted light intensity.

This source of error likely contributed to the wide variance seen in Figure 15. Nevertheless, a weak inverse relationship was observed between the period and the magnitude of the RF field, lending credence to Equation (8).

5 Conclusion

Despite hurdles that negatively impacted the accuracy of the results, the data collected support three claims: first, that the Zeeman splitting is linear with low B (Section 3.2.2); second, that the Zeeman splitting is quadratic with larger B (Section 4.1); and third, that the period of the transient ringing that occurs as the RF field is switched on is inversely related to the magnitude of the RF field.

In the future, the quality of the data could be improved by increasing the period of the square wave modulation of the RF magnetic field. This would give the system more time to reach equilibrium. Additionally, manual calibration should be attempted before measuring the transient phenomena, as the auto-calibrator may not have set the B field to the right value before measurement of the transients began. Time permitting, the collection of more data points would increase the fidelity of the ringing period vs. RF magnetic field amplitude dataset, as well as the quadratic Zeeman effect dataset, which are too sparse to draw any final conclusions.

References

[1] G. Breit and I. I. Rabi. "Measurement of Nuclear Spin". In: *Phys. Rev.* 38 (11 Dec. 1931), pp. 2082–2083. DOI: 10.1103/PhysRev.38.2082.2. URL: https://link.aps.org/doi/10.1103/PhysRev.38.2082.2.

[2] F. D. Colegrove, L. D. Schearer, and G. K. Walters. "Polarization of He^3 Gas by Optical Pumping". In: *Phys. Rev.* 132 (6 Dec. 1963), pp. 2561–2572. DOI: 10.1103/PhysRev.132.2561. URL: https://link.aps.org/doi/10.1103/PhysRev.132.2561.